

# Wide band, ultra low noise cryogenic InP IF amplifiers for the Herschel mission radiometers

Isaac López-Fernández<sup>\* a</sup>, Juan Daniel Gallego<sup>a</sup>, Carmen Diez<sup>a</sup>, Alberto Barcia<sup>a</sup>,  
Jesús Martín-Pintado<sup>a, b</sup>

<sup>a</sup> Centro Astronómico de Yebes, Observatorio Astronómico Nacional, Apartado 148, 19080  
Guadalajara, SPAIN.

<sup>b</sup> currently with Instituto de Estructura de la Materia, Consejo Superior de Investigaciones  
Científicas, Serrano 121, 28006 Madrid, SPAIN.

## ABSTRACT

The sub-millimeter radiometers of the Herschel mission have very stringent requirements. The scientific goals require an instantaneous bandwidth of four GHz with very low noise, flat gain and low power dissipation. Short-term gain stability of the amplifier is important, because gain fluctuations could limit the sensitivity of the instrument. Besides, a highly reliable, low weight unit is required to be compatible with the space instrumentation standards. The amplifiers will be used in conjunction with HEB and SIS mixers in all 7 channels of the instrument. This paper describes the design, the special construction techniques and the results of the amplifiers built by Centro Astronómico de Yebes for the development model of the Herschel Heterodyne Instrument. The average noise temperature obtained in the 4-8 GHz band is 3.5 K, with a gain of  $27 \pm 1.1$  dB at an ambient temperature of 15 K and keeping the total power dissipation below the allowed 4 mW. Normalized gain fluctuations were carefully measured, being lower than  $1.5 \cdot 10^{-4}$  Hz<sup>-1/2</sup> @ 1 Hz. Space qualification of the design is in progress.

**Keywords:** Cryogenic Amplifier, Low Noise, InP HEMT, Gain Stability, Herschel Mission, Sub-millimeter radiometers.

## 1. INTRODUCTION

Cryogenically cooled amplifiers have been routinely used in ground based radio-astronomy receivers for more than 20 years. IF amplifiers as part of millimeter and sub-millimeter receivers have evolved from GaAs Field Effect Transistors (FETs) to GaAs High Electron Mobility Transistors (HEMTs) and more recently to InP HEMTs. During this time, advances in lithography have allowed reduction in the gate length of the devices from 0.5 to less than 0.1 micron. This, together with the progresses in materials and heterostructures has improved greatly the noise temperature performance. However the evolution of the devices have produced the undesired effect of increasing its intrinsic gain fluctuations. The demand of very wide instantaneous bandwidths from the radio astronomers and the extremely low noise temperatures of modern cryogenic amplifiers have made the issue of gain fluctuations more prominent (Wollack<sup>1</sup>).

Herschel mission<sup>2</sup> (formerly known as FIRST) will contain a heterodyne instrument (HIFI<sup>3</sup>) with seven channels of different sub-millimeter receivers, each one with two orthogonal polarizations, in a liquid helium cryostat. The input devices will be either SIS or HEB mixers. As the conversion loss of the mixers can be high, especially in the higher frequency channels, the contribution to the total receiver noise can be significant. The mass of liquid helium in the cryostat is limited, and this imposes a severe limit to the power dissipated inside the cryostat in order to obtain the desired mission lifetime.

The development of the IF amplifiers for Herschel mission was an interesting challenge. In one hand extreme reliability typical of space mission is needed, and in the other hand state of the art noise performance and very low power dissipation are indispensable. Besides, an instantaneous bandwidth of four GHz was a scientific requirement, and low

---

\* isaac@oan.es; phone +34 949 290311; fax +34 949 290063; <http://www.oan.es>; Centro Astronómico de Yebes, Observatorio Astronómico Nacional, Apartado 148, 19080 Guadalajara, SPAIN.

gain fluctuations are needed in order to keep the chopping frequency of the receiver low (Seiffert<sup>4</sup>). The development of the amplifier started building demonstration prototypes with different center frequencies using GaAs HEMTs to demonstrate the viability of the 4 GHz bandwidth, since at that time most radio astronomy receivers used typically no more than 1.5 GHz. Then we realized the impossibility to meet the requirements of noise and power dissipation with the well-established GaAs technology, and the effort was concentrated in InP. As there was no commercial source of InP HEMTs available, we used experimental transistors provided by other groups. Different devices were tested for the production of the different models needed along Herschel program, as they became available. The final decision of the devices to be used for Flight Models (FMs) was based on the performance obtained during the development as well as in the possibility of its space qualification.

Next sections describe the characterization of the devices used, details of the design and construction of the amplifiers and the results obtained. As the data available in the literature on gain fluctuations in cryogenic amplifiers is relatively scarce, it has been considered interesting to pay special attention to this aspect. Detailed data of the measured gain fluctuation of the Development Models (DMs) built is given. Finally, the conclusions of this work are presented.

## 2. DEVICE CHARACTERIZATION

Non-commercial InP technology was selected for the transistors, after a first 8-12 GHz prototype with GaAs commercial devices. The well known advantages of this material at cryogenic temperatures (Pospieszalski<sup>5,6</sup>) are proved true in this frequency range: much lower power consumption at the optimum bias point, almost a factor of two improvement in noise temperature and higher transconductance. Most applications of this material at the time of the beginning of this project took advantage of its high cut-off frequency to produce higher frequency amplifiers. Its use in intermediate frequency (IF) stages brings up stability problems that required a careful design technique.

The transistors S parameters were measured at cryogenic temperatures (13 K) with a HP8510C Vector Network Analyzer (VNA) using an in-house test fixture set with microstrip lines. The devices were mounted and measured with bonding wires in a similar way as they are in the amplifiers. The parameters extracted include the effect of these bonding wires. This test fixture was designed to allow for a cryogenic two-tier TRL calibration (NIST ref.) up to 40 GHz. The process of calibration is very time consuming, as it takes several cool-downs with different line lengths. The values of the elements of the equivalent circuit of the transistor are obtained from DC and S parameters measurements, including coldFET. DC and coldFET allow calculating parasitic elements (Fukui<sup>7</sup>). Intrinsic elements are then determined by optimization using MMICAD<sup>†</sup> Microwave Linear Simulator.

The noise characteristics of the transistors were modeled following Pospieszalski<sup>8</sup>. This model relies only on two parameters or “noise temperatures”: the gate temperature  $T_G$  and the drain temperature  $T_D$ . The first one was assumed equal to the ambient temperature, in our case 13 K. To determine  $T_D$  we used a wide band two-stage test amplifier with an adjustable element, which can easily match transistors of similar gate widths. The DUT is placed in the first stage, while the second stage has a well-known GaAs device. The small signal model of the DUT is included in the amplifier model, and  $T_D$  is chosen to fit the cryogenic noise measurements. The bias of the transistor was selected taking into account not only the noise performance, but also the power dissipation. Each device S parameters must be measured and modeled at several bias points to permit this optimization if no a priori knowledge of the transistor is available.

InP devices of diverse foundries and laboratories (TRW<sup>‡</sup>, ETH<sup>§</sup>), different types and different batches were tested as they became available. We selected devices with 200  $\mu\text{m}$  gate width, whose input impedance levels are easy to match in the wide 4-8 GHz band (the real part is close to 50  $\Omega$ ). We present in fig. 2 the noise and gain results obtained in the test amplifier for the most representative for the project Herschel. ETH 200 T-35 are transistors designed by our request with a layout similar to the GaAs devices we were used to (see fig. 1). Subsequent batches have perfected this design with very successful applications in other amplifiers (López-Fernández<sup>9</sup>). It is not passivated and the gate length is limited to 0.2  $\mu\text{m}$ . This transistor was used in the initial prototypes, but could not be space qualified.

Our laboratories had the opportunity to participate in the Cryogenic HEMT optimization Program (CHOP), led by the Jet Propulsion Laboratory (JPL) and TRW. During the course of this ambitious project TRW foundries produced exceptional cryogenic InP MMICs and HEMT devices with 0.1  $\mu\text{m}$  gate length and susceptible of space qualification.

---

<sup>†</sup> MMICAD v2.18 by Optotek, 62 Steacie Drive, Kanata, Ontario K2K 2A9, Canada

<sup>‡</sup> TRW Inc., Electronic Space & Technology Division, Redondo Beach, CA 90277, USA.

<sup>§</sup> Laboratory for Electromagnetic Fields and Microwave Electronics, Swiss Federal Institute of Technology, Zürich, Switzerland.

The two models shown in fig. 1 have the same gate width (200  $\mu\text{m}$ ) and a similar layout of the active part, but TRW T-39 (IREL1) was fabricated specially for this project with a bigger chip size to facilitate handling and bonding. In spite of the superior performance of TRW T-42 (CRYO3), we choose T-39 for the final version of the amplifiers to assure a high reliability in the mounting process of the FMs in the Spanish industry. Other batches of this model have been tested with similar results (T-45 CRYO4).

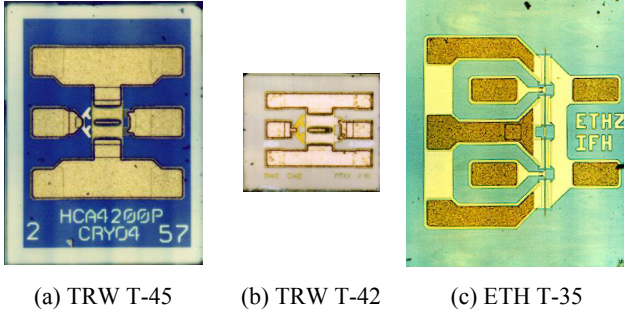


**Figure 1:** Some InP devices tested for this project. Chips are represented in scale; (a) measures 0.33 $\times$ 0.42 mm. (a) and (b) are TRW transistors with 0.1 $\times$ 200 $\mu\text{m}$  gate. (c) is an ETH experimental device with 0.2 $\times$ 200  $\mu\text{m}$  gate used in the MPs. (a) was preferred over (b) for the final DMs due to its bigger chip and pad size, which improves reliability in handling and bonding.

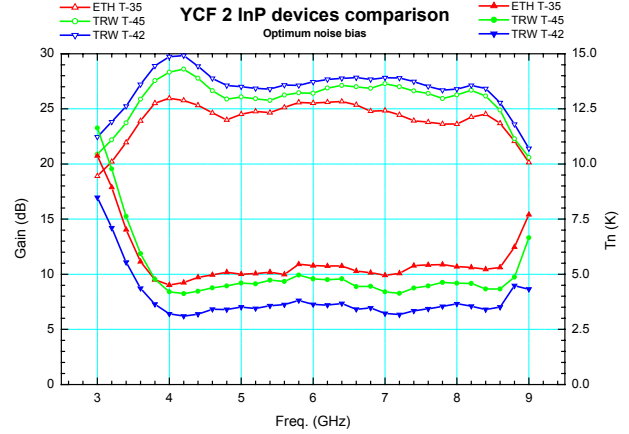


**Figure 2:** Comparison of the characteristics of the transistors presented in fig. 1, at the optimum noise bias in a YCF 2 amplifier.

All other discrete devices used in the amplifiers were carefully selected based on its proper operation at cryogenic temperatures and demonstrated reliability in amplifiers built for ground-based applications over the years. This not only depends on a robust and thermally adequate mechanical design, but certain electrical properties had to be taken into account: for example, some dielectrics may change dramatically at low temperatures making a capacitance drift to zero. Accordingly, cryogenic models of the most critical components had to be established and validated. Nevertheless, for this frequency range only first order effects were finally included in the simulations. The models are made up of concentrated elements (including parasitic resistance and inductance) and do not account for capacitor parallel resonances. We used thick film resistors size 0302 from SOTA\*\* and capacitors form ATC†† of the series 100 (porcelain multilayer) and 111 (parallel plate, with CA dielectric).

### 3. AMPLIFIER DESIGN

The design goals for this project<sup>10</sup> at the operating temperature of 14 K were a very low noise ( $< 5$  K) at low power operation ( $< 4$  mW) with moderate but flat gain ( $> 22 \pm 1.5$  dB) and output return losses ( $< -10$  dB). The difficulties to reach a high reflection coefficient in such a wide band were solved with a PAMTECH‡‡ cryogenic isolator especially developed for this application (see a picture in fig. 3). Therefore, the input return losses only shall be below 0 dB to be compatible with the required unconditional stability. The gain fluctuations must be lower than  $1.4 \cdot 10^{-4} \text{ Hz}^{-1/2}$  but are not considered a design parameter (we believe that it can only be improved by device selection and bias optimization).

The amplifiers were designed using MMICAD. Devices and components are modeled as described in section 2, transmission lines are realized by microstrip circuits and bonding wires are represented by high Z transmission lines. Two stages of InP transistors are sufficient to reach the specified gain. For each one, the transistors are independently stabilized in the band by a resistive loading in drain and an inductive feedback in source. In addition, these elements bring together the minimum noise and input conjugate impedances, and contribute to the gain equalization. The input matching circuit comprises a double quarter wavelength transformer and a high impedance element (bonding wire), to match in the octave band respectively the real and imaginary parts of the minimum noise impedance. The interstage and

\*\* State of the Art, Inc. 2470 Fox Hill Road, State Colledge, PA 16803-1797, USA.

†† American Technical Ceramics, One Norden Lane, Huntington Station, NY 11746-2142, USA.

‡‡ Passive Microwave Technology, Inc. 4053 Calle Tesoro, Camarillo, CA 93012, USA.

output circuits optimize the gain and output reflection. Tuning elements are incorporated in the design in the form of small microstrip islands (around most microstrip lines) and adjustable bonding wires (i.e. an extended gate wire or a double wire to the stabilizing resistor).

The bias networks were designed with several goals in mind: They have to help reaching unconditional stability of the complete amplifier at all frequencies; they should comply with Electromagnetic Compatibility (EMC) requirements of the mission; they must give an effective Electrostatic Discharge (ESD) protection to the extremely sensitive InP devices. Moreover, the voltage drop in the drain lines should be minimized to reduce power dissipation. The last versions include three filtering sections, a voltage divider in the gate lines and a big capacitor acting as a charge divider. Drain resistors were lowered from  $72 \Omega$  to  $49 \Omega$ .

Figs. 4 and 5 show pictures of the amplifiers YCF 2 (ETH transistors) and YCF 6 (TRW transistors). The good model - measurements agreement can be verified in fig. 6.

#### 4. AMPLIFIER FABRICATION

The amplifiers were completely manufactured at the workshops and laboratories of Centro Astronómico de Yebes (CAY). The final FMs will be fabricated by Alcatel Espacio<sup>§§</sup> to meet the stringent specifications in the assembly processes required to qualify the amplifiers for space. The transfer of the technology involved in the construction of cryogenic low noise amplifiers to the industry has finished with success, as demonstrates an Alcatel replica prototype which has already been measured, showing similar performance to CAY-made models.

A total of 37 4-8 GHz amplifiers of different series have been fabricated in Yebes up to now. Table 1 shows how these LNAs were distributed among different projects, institutions and observatories. Amplifiers within a series are identical. We will focus through this and the following sections on series 2 and 6. Series 2 was designed for ETH transistors and was aimed to supply the consortium and specifically, the groups developing the HEB and SIS mixers, with the amplifiers needed in the development phase of the project (the HIFI Mixer Program – MP). Series 6 was a design susceptible of space qualification, incorporating TRW transistors and a mechanical layout compatible with the Focal Plane Unit of HIFI. The DMs delivered to the HIFI Consortium belonged to this series, and are virtually identical to the Qualification and Flight Models that will be made by the industry.

**YCF AMPLIFIERS MANUFACTURED AT CAY**

SERIES	QUANTITY	DESTINATION	SER. NUMBERS
0 - 1	4	Demonstration prototypes for the evaluation of technology, devices and performance	002, 3, 4, 1001
	1	Yebes	2001
	1	Platform for transistor characterization (Yebes)	2010
	8	Herschel MP (SRON, JPL, KOSMA, DEMIRM, Chalmers)	2002-2009
2	4	IRAM ALMA Development	2013, 16, 17, 18
	1	SRON ALMA Development	2015
	4	Harvard-Smithsonian CfA (SMA)	2011, 12, 19, 20
	1	Cambridge Cavendish Laboratory (JCMT)	2014
5	1	Cornell University (Arecibo)	5001
	1	Yebes	6001
6	5	Herschel DMs	6004, 5, 6, 9, 14
	4	Herschel MP (SRON, JPL, KOSMA)	6007, 10, 11, 12
	2	Harvard-Smithsonian CfA (SMA)	6008, 13

**Table 1:** Cryogenic amplifiers designed and built at CAY in the 4-8 GHz band. Series 0, 1 and 2 were designed for ETH transistors (a total of 24 amplifiers). Series 5 and 6 were designed for TRW transistors (a total of 13 amplifiers).

<sup>§§</sup> Alcatel Espacio S.A., Einstein 7, PTM, Tres Cantos, 28760 Madrid, SPAIN.

A PTFE/ceramic composite 20 mils thick with  $\epsilon_r=2.94$  (ROGERS<sup>\*\*\*</sup> RT/duroid<sup>®</sup> 6002) was chosen for the microstrip circuits. The substrates are plated with 6  $\mu\text{m}$  of soft gold and etched in an Iodine bath. The structures (chassis and covers) where the circuits are mounted were milled in a CNC machine. The first series are machined in brass, while series 6 are made in aluminum. This represents an important improvement in terms of mass, and mechanical compatibility. Each piece is gold plated in the same fashion as the substrates to provide corrosion protection and allow for gold wire bonding (aluminum pieces required prior nickel plating). All chassis have two cavities to allocate respectively the signal and bias circuits. Series 6 includes an additional cavity milled on the bottom of the box for additional EMC filters.

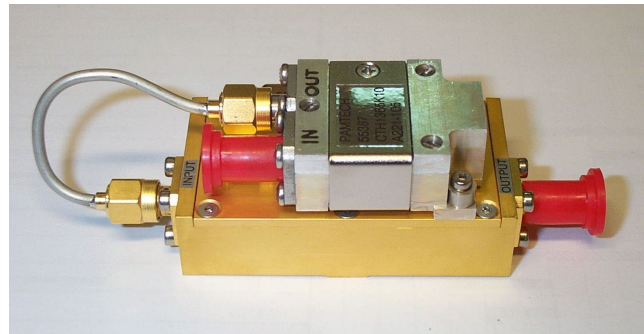


**Figure 3:** One of the first IF amplifier (IF1) units. It comprises a DM amplifier (fig. 6) and a PAMTECH isolator connected to the input via a semirigid coaxial cable

The mounting techniques employed in series 2 are selected by its proven reliability in many past cryogenic designs of CAY, sometimes sacrificing performance. Chip components and substrates are glued to the structure. All interconnections are wire bonded. Nevertheless, series 6 incorporates some improvements. There is a circuit board with the bias/filtering/protection components (in duroid<sup>®</sup> 6002). DC, RF connectors and some chips are replaced by models more reliable or with a higher quality grade. The SMA connector type and bonding procedure offering more guarantees of mechanical stability and good electrical performance, was selected and modeled after an evaluation of several alternatives (Diez<sup>11</sup>). RADIALL 124 501 tab contact is connected to the input line by a loop of gold ribbon welded in the middle to the line and on both ends to the pin to shape an “O” as seen along the connector axis. This gives complete mobility to the connection, avoiding problems of broken contacts when cooled.

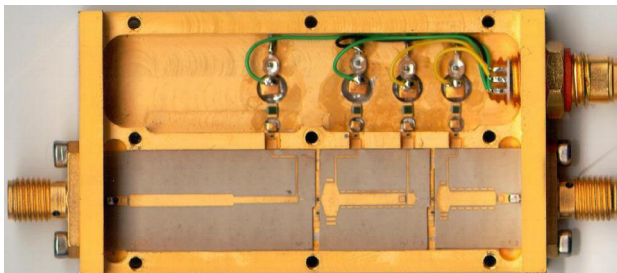


**Figure 4:** YCF 2 amplifiers delivered to the mixer groups. The material used is brass, with a total weight of 149 gr. The external dimensions are 61.4×35×11.5 mm.

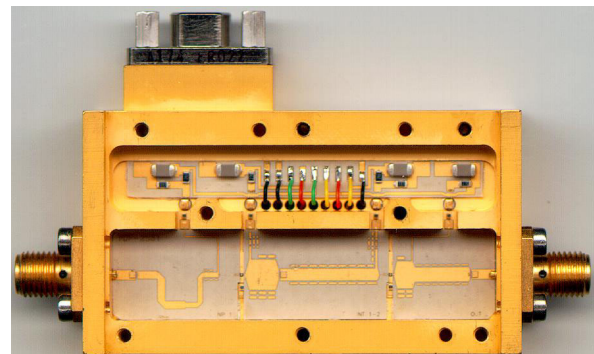


**Figure 5:** YCF 6 amplifiers (Development Models). The material used is aluminum, with a total weight of 65 gr. The external dimensions are 58×32×15 mm. A cavity to allocate additional filtering is machined on the bottom side.

## 5. AMPLIFIER PERFORMANCE

In this section, we will present the test procedures and will discuss the results corresponding to two significant groups of amplifiers (see section 4 and table 1): MP Amplifiers (MPAs) from series 2, with ETH 200 T-35 transistors and the DMs from series 6 with TRW 200 T-39. Our laboratories count with two independent cryogenic measurement systems with very similar in-house test dewars, identified by the closed-cycle helium cryocooler type: CTI 350 for the old low frequency system and CTI 1020 for the last higher frequency one.

<sup>\*\*\*</sup> Rogers Corp. Advanced Circuit Materials Division, 100 S. Roosevelt Avenue, Chandler AZ 85226, USA

The amplifiers are biased with a feedback power supply, which sets the gate voltage for any selected drain current. The bias point of the amplifiers is selected primarily to optimize the noise temperature with the first stage and to reach a compromise between gain flatness and low output reflection with the second stage. The power dissipation limitations imposed by this project difficult the bias optimization process. At the time of measuring the MPAs it was yet unclear the allowed power per amplifier. The results corresponding to this group were obtained at the optimum bias point (about 9 mW, not the same for all the amplifiers). We will comment also on other measurements taken with very low power (less than 3 mW). The DMs are all measured with the same bias:  $V_{D1}=0.85$  V,  $V_{D2}=0.5$  V,  $I_D=3$  mA, (4 mW dissipated in the amplifier, compliant with the latest specifications). Note that the drain series resistance is  $72 \Omega$  for the MPAs and  $49 \Omega$  in the DMs.

### 5.1 Noise and gain measurements

All cryogenic measurements were taken in the 350 system following the cold attenuator method<sup>12</sup>. This system is based in a computer controlled HP8970B Noise Figure Meter and includes a modified HP8971C test set with an external MITEQ preamplifier, an HP83650B sweeper and auxiliary equipment to acquire temperature and bias data. Hot and cold loads are implemented by a 15 dB ENR HP346C noise diode (at room temperature), plus a 15 dB attenuator and a DC-block (NARDA) inside the cryostat. The DC-block is used to avoid heating the active part of the attenuator by the inner conductor of the stainless steel coaxial line. The absolute system accuracy for the noise temperature range of these amplifiers has been estimated in  $\pm 1.4$  K ( $3\sigma$ ) with repeatability better than this value by an order of magnitude (Gallego<sup>12</sup>).

Fig. 6 shows the results of the MPAs and DMs respectively. To avoid cluttering the graph with too many traces, a colored band represents the area where all the individual amplifier measurements for each variable are confined. The solid curve corresponds to the average of all the amplifiers. The outcome of the model simulations is plotted for comparison. Table 2 summarizes these plots in figures. It is notable the consistency of low noise results, with an average of 3.57 K for all DMs. The dispersion of the curves is greater for the DMs in gain due to the tuning processes in the second stage to improve gain flatness, while dispersion in noise is greater for the MPAs because the individual bias optimization did not lead to the same polarization for each one. The consequences of selecting the low bias point for the MPAs are a degradation of 0.5 K in noise and a reduction of 2.5 dB in gain. The limitation of 4 mW in the bias of the DMs has a small impact in noise if we sacrifice the performance of the second stage. With only 3 mA of drain current, TRW transistors are a few tenths of K over their optimum noise. The impact of the isolator on the noise temperature of the amplifier is described in detail in section 5.4 (see table 4). For the isolators measured, the average noise degradation expected from loss measurements is between 0.8 K and 1.5 K.

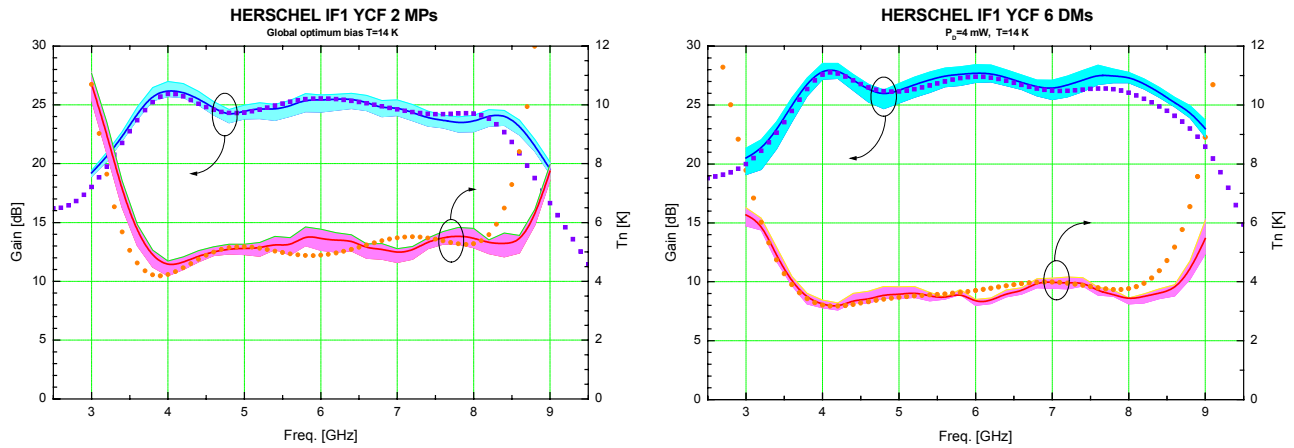


**Figure 6:** Gain and noise of the MPAs (on the left, 8 LNAs with ETH experimental transistors) and the DMs (on the right, 5 LNAs with TRW transistors). The colored bands are defined by worst and best values for all the amplifiers. The solid line is the average of the series. The dots correspond to the noise model and the squares to the gain model.

AMPLIFIER GROUP	NOISE TEMPERATURE [K] (MEAN)			GAIN [dB] (MEAN)			GAIN FLATNESS [dB] (PEAK TO PEAK)		
	Best amp.	Average	Worst	Best amp.	Average	Worst	Best amp.	Average	Worst
YCF 2 MPAs	4.89	<b>5.18</b>	5.38	25.29	<b>24.80</b>	24.06	2.35	2.85	3.19
YCF 6 DMs	3.46	<b>3.57</b>	3.72	27.70	<b>27.11</b>	26.26	1.96	2.19	2.46

**Table 2:** Noise and gain performance at 14 K of the two groups of amplifiers delivered to the consortium. Mean and peak to peak values are calculated for the 4-8 GHz band. Note the improvements in the final DMs due to the perfected design and superior transistors. It is remarkable the repeatability of each series.

Noise measurements of two representative amplifiers were repeated in system 1020, using the same procedure. The results are slightly better, within the error budgets of both systems. The noise temperature is 0.75 K lower in average (the difference increase with frequency) and the ripples in the gain are significantly reduced (0.8 dB smaller peak to peak values). Extrapolating these findings and the results of the transistor comparison of section 2 to an YCF 6 amplifier with a TRW 200 T-42 transistor in the first stage, we could expect measuring in system 1020 *average noise temperatures in the 4-8 GHz band in the order of 2 K*. The differences between both test sets are not very important. We believe that the origin of the discrepancy may be in the older calibration of 350 components (lines, temperature sensors) and the linearity of the detectors in the receiver. The comparison for one of the amplifiers can be seen in fig. 7. Note how 1020 noise traces look neater, freer of spurious ripples.

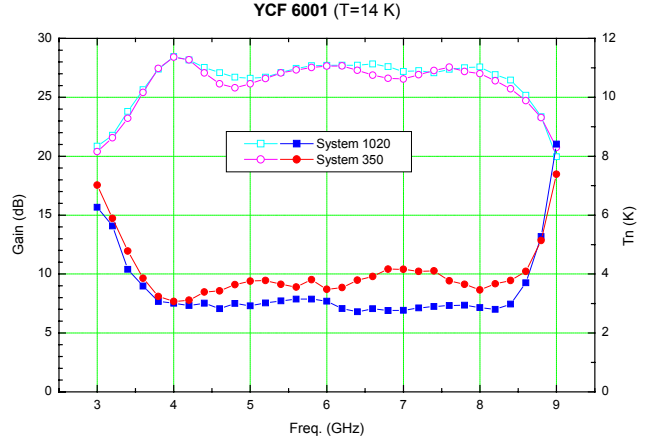


**Figure 7:** Comparison of noise and gain measurements of an amplifier in the two systems available at CAY. All noise data presented in this paper correspond to the older system 350, chosen to maintain the comparability with past measurements.

## 5.2 Gain fluctuations measurements

The issue of gain stability in cryogenic amplifiers has been addressed previously by Wollack<sup>1</sup>, Jaroski<sup>13</sup>, Kooi<sup>14</sup> and Seiffert<sup>4</sup> among others. Our aim in this paper is to add some more data to the values existent in the literature. Gain fluctuation data was only taken systematically for the DMs (with TRW transistors). In principle the larger gate area of ETH devices should yield lower fluctuations, but other factors like passivation, materials and bias points may have a larger contribution.

We have opted to characterize this parameter by the spectral density of normalized gain fluctuations. The measurements were performed using the available equipment at our laboratory. Data was taken at a single frequency (6 GHz) using a continuously variable attenuator, air lines and the HP8510C VNA, according to Gallego<sup>15</sup>. Several spectrums, in the range 0.012-2.34 Hz, are obtained by Fast Fourier Transform of the VNA time domain data and averaged to reduce random fluctuations. The contribution of the system fluctuations is subtracted from the measurements. The spectral density of the fluctuations in HEMT amplifiers in the frequency range where 1/f noise dominates follows a general expression of the form

$$S(f) = \beta \cdot \left( \frac{1 \cdot \text{Hz}}{f} \right)^{\alpha/2}, \quad (1)$$

The reference value used to compare different amplifiers is the fluctuations at 1 Hz ( $\beta$ ), expressed in 1/ $\sqrt{\text{Hz}}$  (when the spectral index  $\alpha$  is 1). It is calculated together with  $\alpha$  fitting equation 1 to one decade of data between 0.1 and 1 Hz (very low frequency points are more sparse and unreliable). One example of this measurement is shown in fig. 8. All the data presented is taken at 14 K. Room temperature data is limited in some cases by the sensitivity of our system. Table 3

contains the results for all the DMs. The fluctuations at 1 Hz averaged for the 5 amplifiers are  $9.4 \cdot 10^{-5} \text{ Hz}^{-1/2}$ . The spectral index is smaller than reported in the literature (Wollack<sup>1</sup>), however the available frequency range for our fitting was small.

A peak usually appears at 1 Hz due to the cycle of the CTI 1020 refrigerator. There is a strong relation between the intensity of this peak and the position and way of attaching the amplifier to the cold plate; for certain arrangements we have been able to reduce it below the noise level (Risacher<sup>16</sup>). It is clear that the origins of this perturbation are in thermal oscillations and/or acoustic vibrations in the amplifier (Kooi<sup>14</sup>). We have verified the first hypothesis increasing the thermal load of the cold stage (we detached the thermal links of several transition lines to the intermediate stage); the peak grows as a result of the greater heat flux through the amplifier, placed right over the refrigerator head.

AMPLIFIER YCF	GAIN FLUCT. @ 1Hz ( $\beta$ )	SPECTRAL INDEX ( $\alpha$ )
6004	8.62E-05	0.754
6005	8.88E-05	0.706
6006	1.29E-04	0.562
6009	1.00E-04	0.726
6014	1.02E-04	0.762
<b>Average</b>	<b>9.40E-05</b>	<b>0.737</b>

**Table 3:** Gain fluctuation data from the DMs at 14 K according to equation 1. YCF 6006 amplifier is a pathological case with inverted slope at room temperature, not included in the average.

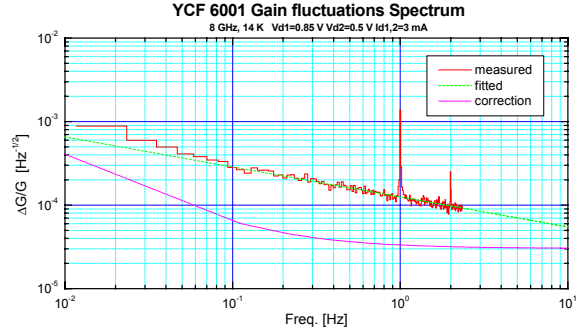


**Figure 8:** Example of the typical spectral density of normalized gain fluctuations data obtained after processing the VNA measurements. Note the peak at 1 Hz (see text).

We also measured in some amplifiers the gate voltage fluctuations with an HP35670A Dynamic Signal Analyzer, to verify the correlation between bias and gain fluctuations. It must be reminded here that the power supply used adjusts the gate voltage to maintain constant the selected drain current with a loop bandwidth of some 100 Hz. We have verified that this approach yields slightly better results than keeping a constant gate voltage (Jaroski<sup>13</sup>). The gate voltage is therefore the most accessible bias parameter, but within the servo bandwidth we will actually be testing the drain current fluctuations. We first took a set of measurements of the gate voltage noise of different amplifiers at the same bias point. The reference parameter is the absolute fluctuations at 1 Hz, in  $\text{V}/\sqrt{\text{Hz}}$ . Fig. 9 shows a moderate correlation between these values and the measured gain fluctuations. Then, we studied the variation of the gate and gain fluctuations with the bias point. We measured both parameters sampling several drain voltages while keeping a fixed drain current. The reference parameter for the voltage fluctuations is now at 10 Hz to be above the white noise level for low drain voltages. It was observed a significant steep variation of almost one decade in the gain fluctuations for a  $V_D$  excursion of 0.15 V (under these conditions other parameters, as noise or gain hardly change). We had seen clues of this phenomenon in other amplifiers. A similar behavior is measured in the voltage fluctuations but with a less sharp slope (see fig. 10). Again it is clear that a correlation exists between  $V_G$  noise and gain fluctuations, now for different bias points of the same amplifier (fig. 11).

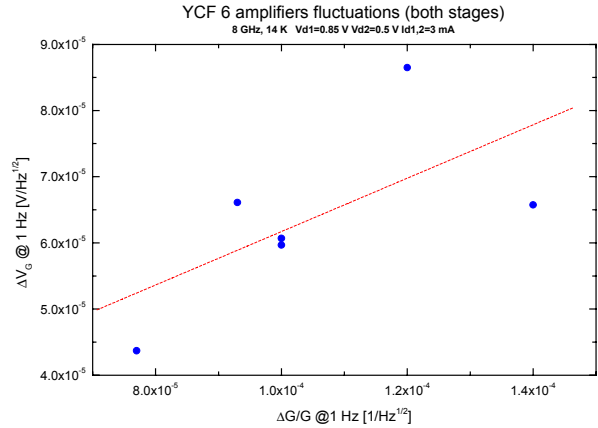


**Figure 9:** Gain fluctuations versus gate voltage fluctuations for 6 DM amplifiers measured at the same bias point. Gate fluctuations are defined as  $\sqrt{\Delta V_{G1}^2 + \Delta V_{G2}^2}$ . Note the significant correlation.

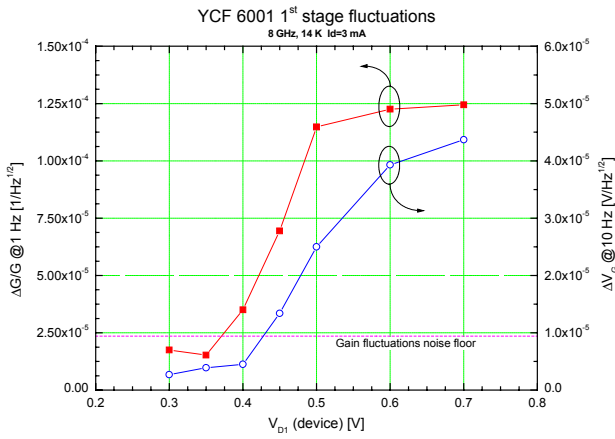


**Figure 10:** Dependence of the gain and gate voltage fluctuations of an amplifier on the drain voltage. Note the steep change for  $V_D < 5$ . The values of the gain stability for the lowest drain voltages are contaminated by the system noise.

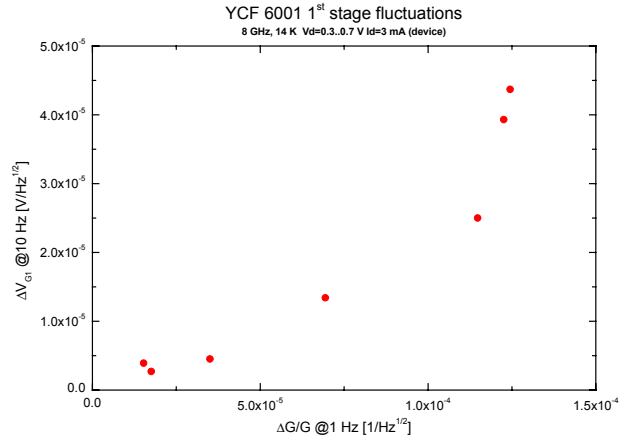


**Figure 11:** Gain fluctuations versus gate voltage fluctuations of the 1<sup>st</sup> stage of an amplifier for different drain voltages. A correlation is apparent. The data corresponds to fig. 10.

This relationship between bias noise and gain fluctuations could be useful to select the best individual devices of a batch in terms of gain stability with simple DC measurements. As practical conclusions from these measurements, the dispersion of gain fluctuations of the amplifiers is higher than in noise temperatures. That makes individual characterization very important. Special attention should be paid to the bias point. It is easy to enter in a region of high fluctuations when optimizing other characteristics. The measurement of fluctuations in gate voltages could be used to easily detect the high fluctuation zones.

### 5.3 Reflection and stability measurements

Routine cryogenic reflection (and gain) measurements of the amplifiers were done in system 350 with an HP8757A Scalar Network Analyzer (SNA) in AC mode. The same system in DC mode is used to detect possible oscillations up to 26 GHz. This is a very effective and sensitive way to detect oscillations even at frequencies exceeding the maximum specified for the detector used. An Agilent 9565EC spectrum analyzer can help finding higher frequency oscillations, not uncommon in transistors with such cut-off frequencies. Exceptionally, amplifier S parameters were measured more carefully in the HP8510C VNA, using the de-embedding and time domain gating techniques described in section 5.4. The superior accuracy of the more sensitive VNA does not introduce important corrections to the SNA results, although some differences appear due to the effects of the transitions and cables in system 350. The value of K (Rollet stability factor) obtained from S parameter measurements also shows good agreement with the model results.

All amplifiers are unconditionally stable for a broad range of bias points around the optimum used in normal operation (all combinations of input and output impedances are checked connecting sliding shorts to the input and output ports of the dewar). The output reflection coefficient is usually the parameter with a poorer prediction from our models. Nevertheless, the results are satisfactory. The MPAs yield an average of the lowest in-band reflection coefficient for the 8 amplifiers of  $-14.3$  dB. There is a slight improvement of  $0.5$  dB when biasing these amplifiers at the low dissipation point. For the DMs this value is  $-13$  dB (the return losses at the high end of the band were sacrificed for a better gain flatness). Fig 12 illustrates these results in a similar style as the gain and noise plots. The tuning of the intermediate and output matching circuits to improve gain flatness is responsible of the bigger dispersion of the output return losses of the DMs.

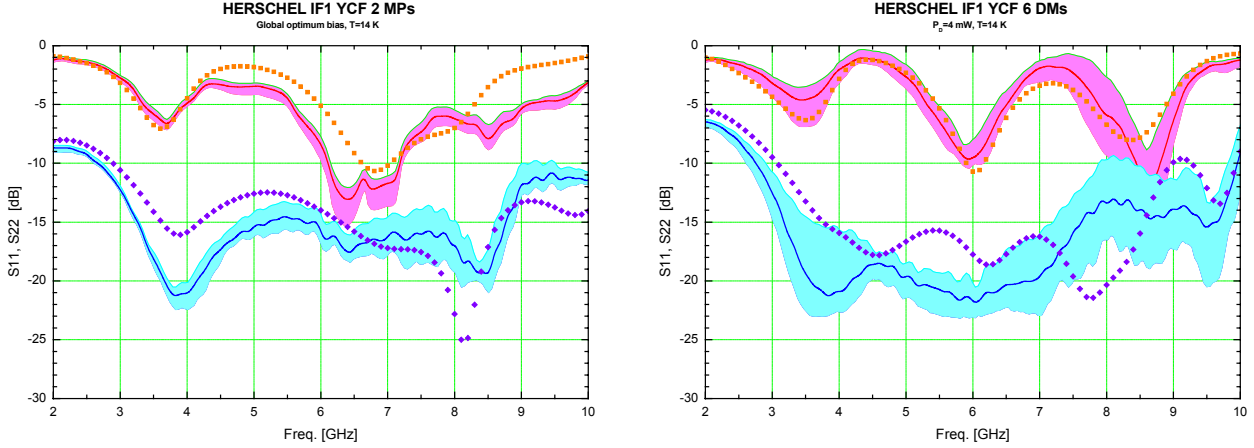


**Figure 12:** Reflection measurements of the MPAs (on the left, 8 LNAs with ETH experimental transistors) and the DMs (on the right, 5 LNAs with TRW transistors). The input reflection was not a design parameter for these amplifiers. The colored bands are defined by worst and best values for all the amplifiers. The solid line is the average of the series. The dots correspond to the input coefficient model and the squares to the output coefficient model.

#### 5.4 Isolator measurements

Our group has delivered amplifiers with two models of PAMTECH isolators. CTH1365 K4 (9 isolators) was for the YCF 2 MPAs. CTH1365 K10 (5 isolators) is a variant of K4 with some mechanical modifications to fit in the mixer subassembly, and an attempt to center the band at 14 K. It is the isolator used in the DMs and will be qualified for the FMs. PAMTECH only characterizes the isolators at 77 K. We have tested each isolator at 14 K in our 1020 system with a setup described in detail in Gallego<sup>16</sup>. The S parameters measurements were performed with the HP8510C VNA. A full two-port calibration was done with reference planes at the end of the flexible cables of the VNA, outside the dewar. The home-made stainless steel coaxial air lines transitions were measured independently at ambient temperature, and their effect was de-embedded in the post-processing of the data (their S parameters change very little with temperature). A time domain gate was applied to reduce the reflection originated by the semi-flexible cable connecting the output of the isolator with the dewar transition. The cryogenic loss of this line is part of the measured S21 (the estimated contribution is only 0.08 dB @ 8 GHz).

The excellent results obtained for all model K10 isolators with this procedure are given in fig. 13. Table 4 summarizes the averages, best and worst cases for the worst values of the S parameters at 14 K in the band. The isolation and reflection of model K10 are worse probably due to an overcorrection in the band shift requested after the measurement of model K4 (the degradation occurs at high frequencies). On the contrary, the isolation improves.

The increment in noise temperature  $\Delta T_c$  produced by an isolator connected to the input of an amplifier is given by<sup>17</sup>

$$\Delta T_c = \left( \frac{1}{G_{iso}} - 1 \right) \cdot (T_{amb} + T_{amp}), \quad (2)$$

where  $T_{amb}$  is the physical temperature of the isolator,  $T_{amp}$  is the equivalent noise temperature of the amplifier and  $G_{iso}$  is the available gain of the isolator, and can be formulated in terms of the measured S parameters as

$$G_{iso} = \frac{|S_{21}|^2}{1 - |S_{22}|^2}. \quad (3)$$

These expressions are used to calculate the contribution to the noise temperature of the cascaded isolator and amplifier showed in table 4. The amplifier is supposed to have 3.6 K of noise and the isolator to be at 17 K ambient temperature. There is a good agreement with actual measurements of a complete IF1 unit (the ensemble of a pre-amplifier, an isolator and the interconnect cable, see fig. 3). The mean insertion losses across the band averaged for all the isolators measured are 0.20 dB for K4 and 0.30 dB for K10. The mean noise temperature increment is 1.12 K for K4 and 1.38 K for K10.

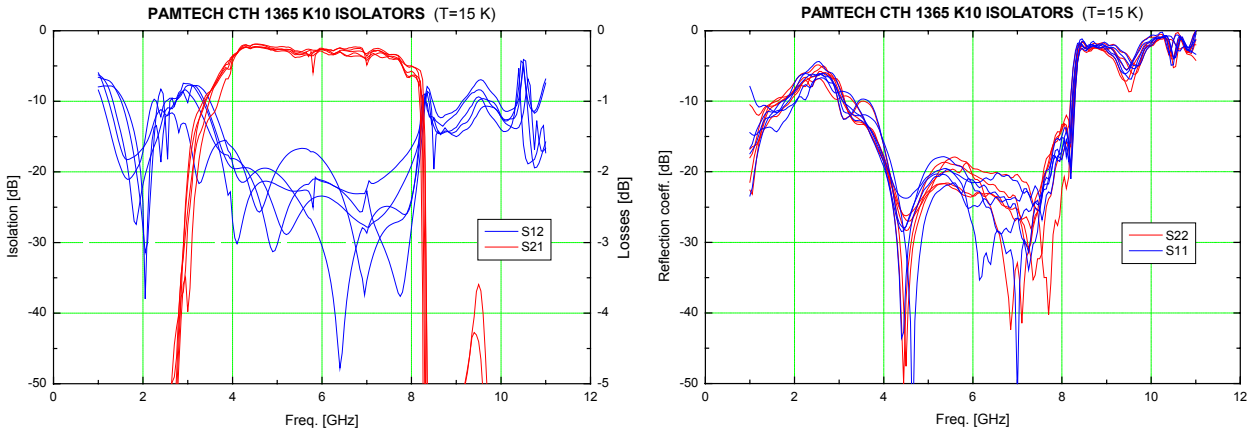


**Figure 13:** S parameter measurements of the 5 PAMTECH 1385 K10 isolators used in combination with the DMs. The dips in S21 are not artifacts. The limiting points for the worst values of table 4 are always at 8 GHz.

### PAMTECH CRYOGENIC ISOLATOR MEASUREMENTS

ISOLATOR MODEL	DATA TYPE	MEASUREMENTS @ 14 K [dB]				$G_{av\ mean}$ [dB]	$\Delta T_{c\ mean}$ [K]
		$S_{11} <$	$S_{22} <$	$S_{12} <$	$S_{21} >$		
CTH1365 K4	Best of 9	-19.6	-19.0	-19.6	-0.27	-0.17	0.81
	Average	<b>-18.8</b>	<b>-18.1</b>	<b>-17.4</b>	<b>-0.36</b>	<b>-0.20</b>	<b>1.12</b>
	Worst of 9	-18.2	-17.3	-16.0	-0.46	-0.30	1.48
CTH1365 K10	Best of 5	-18.0	-17.9	-20.7	-0.50	-0.26	1.25
	Average	<b>-16.2</b>	<b>-15.4</b>	<b>-18.3</b>	<b>-0.58</b>	<b>-0.28</b>	<b>1.38</b>
	Worst of 9	-15.0	-14.0	-16.5	-0.66	-0.30	1.47

**Table 4:** Summary of the results for the two models of isolators measured. The best and worst cases and the average for all the isolators of the worst value of each S parameter in the band is presented. The measurement procedure is not exactly the same for both models<sup>†††</sup>. The last two columns are the calculated mean insertion losses and the estimated noise contribution (see text).

## 6. CONCLUSIONS

A total of 34 cryogenic InP HEMT amplifiers with different designs in the 4-8 GHz band were fabricated during the development phase of project Herschel. We present the results of two series delivered to the consortium, one with ETH experimental devices and another with TRW devices. The transistors S parameters were measured at cryogenic temperatures and cryogenic noise models were developed with the aid of a test amplifier. The last series (Development Models), demonstrate an exceptional performance with just 4 mW of dissipated power, with a mean for all the amplifiers of 3.58 K of noise and  $27.1 \pm 1.1$  dB of gain averaged in the band, and an excellent repeatability. The use of cryogenic isolators from PAMTECH at the input allows for a wide band, mixer-independent design but with a mean penalty in noise of 1.1 – 1.4 K. Measurements of gain fluctuations exhibit a greater dispersion and a very acute sensitivity to the bias point. It was found that an a priori selection of devices in terms of gain fluctuations might be done measuring the low frequency noise of the gate bias and, furthermore, the bias regions of high fluctuations could be detected by the measurements of this parameter.

<sup>†††</sup> Model K4 was data was obtained without performing the de-embedding of the cryostat input and output lines and instead normalizing S21 and S12 respect to the value of a short, low loss, U-shaped cable connecting input and output ports inside the dewar. This introduces minor perturbations in input and output reflection and tiny insertion losses ripples.

## ACKNOWLEDGEMENTS

This research was supported in part by the Spanish Administration grants ESP2001-4519-PE (Ministerio de Ciencia y Tecnología), ESP99-1291-E (Acción Especial CICYT-PNIE) and ESP97-1688-E (Acción Especial CICYT-PNIE), and the European Commission project 1FD1997-1442 (CICYT-FEDER). TRW InP transistors used in this project were developed in the Cryogenic HEMT Optimization Program funded under NASA Code R Enabling Concepts and Technologies Program. The authors would like to thank Richard Lai and Ronald Grundbacher of TRW and John C. Pearson and Todd C. Gaier of JPL for the contribution to the definition of the devices finally chosen and for providing all the transistors for the experiments and the final amplifiers. They also acknowledge Otte J. Homan of ETH for providing the experimental devices used in the MPAs. Rafael García and Daniel Geijo are responsible of the fine technical work done for the manufacture of the amplifiers.

## REFERENCES

1. E. J. Wollak, M. W. Pospieszalski, "Characteristics of broadband InP millimeter-wave amplifiers for radiometry", *IEEE MTT-S Int. Microwave Symp. Digest.*, 1998.
2. G. Pilbratt ed., *FIRST – Far Infrared and Submillimeter Telescope*, ESA SCI(93)6, 1993.
3. N. D. Whyborn, "A Heterodyne Instrument for FIRST: HIFI", *Proc. 30<sup>th</sup> ESLAB Symp., Submillimeter and Far Infrared Space Instrumentation*, ESTEC, Noordwijk, The Netherlands, Sep. 1997.
4. M. W. Pospieszalski, "Cryogenically-Cooled, HFET Amplifiers and Receivers: State-of-the-Art and Future Trends", *IEEE MTT-S Int. Microwave Symp. Digest.*, 1992.
5. M. W. Pospieszalski, L. D. Nguyen, M. Lui, T. Lui, M.A. Thompson, M. J. Delaney, "Very low noise and low power operation of cryogenic AlInAs/GaInAs/InP HFET's", *IEEE MTT-S Int. Microwave Symp. Digest.*, 1994
6. H. Fukui, "Determination of the basic device parameters of GaAs MESFET", *Bell System Tech. J.*, vol. 58, pp.771-797, Nov. 1979.
7. M. W. Pospieszalski, "Modeling of Noise Parameters of MESFET's and MODFET's and Their Frequency and Temperature Dependence", *IEEE Trans. Microwave Theory Tech.*, vol. 37, pp. 1340-1350, Sep. 1989.
8. I. López-Fernández, J. D. Gallego, O. J. Homan, A. Barcia Cancio, "Low-Noise Cryogenic X-Band Amplifier Using Wet-Etched Hydrogen Passivated InP HEMT Devices", *IEEE Microwave Guided Wave Lett.*, vol. 9, pp. 413-415, Oct. 1999.
9. Th. De Graauw, *Heterodyne Instrument for FIRST, A proposal to the European Space Agency, Part I: Scientific and Technical Plan*, 1998.
10. C. Diez, J. D. Gallego, I. López-Fernández, R. García, "Electrical characterisation of SMA connectors for cryogenic amplifiers", *Technical Report CAY 2000-6*, Nov. 2000.
11. J. D. Gallego, I. López-Fernández, "Definition of performance of X band cryogenic amplifiers", *Technical Note ESA/CAY-01 TN01*, Jul. 2000.
12. J. D. Gallego, I. López-Fernández, "Measurements of gain fluctuations in GaAs and InP cryogenic HEMT amplifiers", *Technical Report CAY 2000-1*, Feb. 2000.
13. C. Risacher, V. Belitsky, "Low noise cryogenic IF amplifiers for Super Heterodyne Radioastronomy Receivers", *13<sup>th</sup> Int. Symp. Space Terahertz Tech.*, Boston, Mar. 2002.
14. J. W. Kooi, G. Chattopadhyay, M. Thielman, T. G. Phillips, R. Schieder, "Noise stability of SIS receivers", *Int. J. Infrared Millimeter Waves*, vol. 21, pp 689-716, 2000.
15. N. C. Jaroski, "Measurements of the Low-Frequency-Gain fluctuations of a 30-GHz High-Electron-Mobility-Transistor Cryogenic Amplifier", *IEEE Trans. Microwave Theory Tech.*, vol. 44, pp. 193-197, Feb. 1996.
16. J. D. Gallego, "Cryogenic measurements of amplifier YCF 6005 with isolator CTH1365K10 A151-101", *HIFI-FPSS-IF1 Technical Note Yebes/FPSS/TN/2002-003 Issue 2*, Jun, 2002.
17. M. D. Seiffert, J. D. Gallego, I. López-Fernández, N. D. Whyborn, J. C. Pearson, "IF amplifier stability for the Heterodyne Instrument for FIRST", *UV Optical and IR Space Telescopes and Instruments*, Proc. SPIE vol. 4013, 2000.